J Musculoskelet Neuronal Interact 2013; 13(2):166-177

Original Article

Hylonome

# Bone and muscle structure and quality preserved by active versus passive muscle exercise on a new stepper device in 21 days tail-suspended rats

**L-W. Sun[1†], D. Blottner[2†], H-Q. Luan[1], M. Salanova[2], C. Wang[1], H-J. Niu[1], D. Felsenberg[3], Y-B. Fan[1]**

[1]Key Laboratory for Biomechanics and Mechanobiology of Ministry of Education, School of Biological Science and Medical Engineering, Beihang University, Beijing 100191, China; [2]Department of Vegetative Anatomy and Center of Space Medicine Berlin, Neuromuscular Group, Charité University Medicine Berlin, Freie und Humboldt Universität Berlin, Campus Mitte, 10115 Berlin, Germany; [3]Center of Muscle and Bone Research, Charité University Medicine Berlin, Campus Benjamin Franklin, 12200-Berlin, Germany
†First co-authors: Lian-Wen Sun, Dieter Blottner

**Abstract**

Human performance in microgravity is characterized by reversed skeletal muscle actions in terms of active vs. passive mode contractions of agonist/antagonist groups that may challenge principal biodynamics (biomechanical forces translated from muscle to bone) of the skeletal muscle-bone unit. We investigated active vs. passive muscle motions of the unloaded hindlimb skeletal muscle-bone unit in the 21 days tail-suspended (TS) rat using a newly designed stepper exercise device. The regimen included both active mode motions (TSA) and passive mode motions (TSP). A TS-only group and a normal cage group (CON) served as positive or negative controls. The muscle and bone decrements observed in TS-only group were not seen in the other groups except TSP. Active mode motions supported femur and tibia bone quality (5% BMD, 10% microtrabecular BV/TV, Tb.Th., Tb.N. parameters), whole soleus muscle/myofiber size and type II distribution, 20% increased sarcolemma NOS1 immunosignals vs. CON, with 25% more hybrid fiber formation (remodeling sign) for all TS groups. We propose a new custom-made stepper device to be used in the TS rat model that allows for detailed investigations of the unique biodynamic properties of the muscle-bone unit during resistive-load exercise countermeasure trials on the ground or in microgravity.

**Keywords:** Bone Loss, Skeletal Muscle Atrophy, Spaceflight Analogue, Countermeasure, Rat, Biomechanics

## Introduction

In human spaceflight, resistive exercise regimen is considered as effective prescriptions to minimize the risks of microgravity-induced musculoskeletal system impairments, psychological problems (depression), and cardiovascular insufficiencies[1-5]. The unique biodynamic properties (i.e., biomechanical translational forces from muscle to bone) of the deconditioned human musculoskeletal system to exercise stimulation and thus efficacy of exercise-driven countermeasure protocols for the human body in microgravity are however less well understood compared to the well-studied biomechanical or functional properties of the human musculoskeletal system on Earth.

Human performance on the ground is principally characterized by alternating active and passive motion phases[6]. In active motions, the muscle contracts volitionally to overcome resistance caused by one's own body weight, whereas in passive motions, external forces from the training device or even manpower itself help to counteract the resistance in such a way that translation of the biomechanical forces from muscles to bone (i.e., biodynamics) will be considerably reduced if not negligible. For example, passive motions are performed in routine clinical hip joint tests and passive knee extensor stretching to overcome constrained joint movements or to offset muscle fatigue/stiffness in sports. Thus, relatively low mechanical loading of the muscle-bone interface will be produced by passive motions controlled by the sportsman himself or his/her physiotherapist.

The authors have no conflict of interest.

*Corresponding author: Yubo Fan, PhD & Prof., Key Laboratory for Biomechanics and Mechanobiology of Ministry of Education, School of Biological Science and Medical Engineering, Beihang University, Beijing 100191, China*
*E-mail: yubofan@buaa.edu.cn*

*Edited by: S. Warden*
*Accepted 19 April 2013*

Both working load and power/force are major functional determinants supporting the musculoskeletal apparatus in terms of a 1G-adapted physiologically bone-string (string=muscle-tendon unit) interplay in normal human movement and sports. In space, absence of gravitational load (μG) though mimics "an invisible hand" that virtually assists an astronaut's performance working against resistance forces produced by mechanical loading during routine work and performance. Due to altered mass inertia in microgravity repetitive bouts on presently used countermeasure devices[7] may likely also result in considerably altered motion patterns of a normal leg muscle and its antagonist counterpart with respect to a reversed push-pull motion of flexor and extensor leg muscle groups following e.g., ergometer cycling in space even if similar gravitational load is provided by the device in microgravity. As a consequence, reversed activity patterns of closed vs. open chain muscles are apparently initiated during on-orbit exercise regimen that might produce some aberrant biomechanical stress of the Astronaut's joint-bone-muscle interface in a given motion body segment while the outcome of such adverse biodynamical stress on structural and functional properties of the muscle-bone unit following physical exercise countermeasure in spaceflight are presently largely unknown.

Evenmore, most of the astronaut's preflight training on the ground or even the routinely prescribed inflight countermeasure protocols on orbit include more or less strenuous resistive exercise regimens with repetitive bouts routinely and frequently used by various athletes in sports to improve neuromuscular power and force during their competitions on the ground. However, the unique biodynamic demands of the deconditioned human muskuloskeletal system on orbit are difficult to be studied in astronauts due to the known mission constraints (e.g., compliance with exercise). Recent inflight data of on-orbit exercise protocols, for example, showed that astronauts on the International Space Station (ISS) performed on-orbit training but without the expected positive training effects on structural and functional muscle or bone parameters[7-10]. As a consequence, more detailed protocol monitoring such as compliance with exercise prescriptions and increase in duration and working load were proposed to further improve efficacy of inflight countermeasure protocols[11,12]. If the outcome of presently onboard exercise countermeasure protocols performed in microgravity were, at least partly, also due to possible altered biodynamic properties of the muscle-bone interface in microgravity has not been elaborated so far.

We used the tail-suspended (TS) rat model, an accepted rodent experimental analog to human spaceflight, for principal investigations on active muscle contractions induced by spontaneous muscle contractions by controlled plantar electrical impulse activation, and compared them to passive muscle contractions triggered by passive hind limb lifting[13] using a newly custom-made exercise stepper device for active vs. passive mode leg motions in rodents thereby modeling biomechanical stress parameters induced by altered movements following hind limb-unloading on the ground. Our major aim was to provide pertinent evidence for distinct qualitative and quantitative training effects on principal bone and muscle properties.

## Materials and methods

**Experimental animals and animal care.** Female 8-week-old Sprague Dawley rats were purchased from Experimental Animal Center of Beijing University (body weight ranged 215 to 235 g). After one week of adaptation to standard laboratory cages (n=2, each cage), twenty animals (n=20) were randomly selected and divided into four groups (n=5, each): tail-suspension (TS), tail-suspension plus active exercise (TSP), tail-suspension plus passive motion (TSP) and a control (CON) group. In TS, TSP and TSA, rats were subjected to tail suspension for a duration of 21 days of hind limb unloading[14]. While tail-suspended, the TSP and TSA rats were subjected individually to either passive mode motion or active mode exercise induced by a custom made TS-rat training device designed in our laboratory (Figure 1). All TS-rat groups including CON were subjected to the same nursery/housing conditions with 12h dark-light cycles and food and water *ad libitum* for 21 days in the animal facility of the Department at Beihang University, China. Animal treatment and care was according to Regulations for the Administration of Affairs Concerning Experimental Animals promulgated by Decrete No.2 of the State Science and Technology Commission of China and the Guiding Principles for the Care and Use of Animals approved by Beijing Government. All protocols were approved by the Animal Care Committee of Beihang University, China.

**Exercise training with a stepper device.** We designed a novel exercise stepper training device for active and passive mode training protocols for TS-rats as shown in Figure 1. Briefly, the rat's trunk was placed in a fixed box (30° angle) while its tail was suspended via fixation to an overhead TS crossbeam. The rat's left and right rear feet were taped on the stepper footplates with medical adhesive tape. While suspended, the rat's body maintained a head down tilt angle of 30° to secure for complete hindlimb unloading. Active mode leg motion: When active mode exercise was performed, the training was started by the pulse electrical arc stimulator as previously reported[15]. Electric impulse-induced reflexive muscle activation of the left and right rear leg was alternately achieved by electrodes applied to the footplate in such a way that a short voltaic arc (>1000 V, 200 ms) was produced adjacent to the plantar region without direct electrode contacting on the skin thereby inducing uncomfortable skin sensation on the foot paw. Active leg motions in the conscious TS rat was induced spontaneously and alternately to the rear feet without direct stimulation of a given nerve or a hind leg muscle group. As a consequence, the TS-rat always actively moved its left or right hind limb in an alternating pattern together with the two adjacent foot stepper pedals. Each impulse resulted in active leg muscle contractions (variantly in one left and one right leg) as monitored by EMG and each active bout was considered as being part of resistive load training as the rat hind limb muscles needed to overcome a load of 0-4 N (Figure 1C) produced by a spring fixed between pedal and bottom plate of the device that, in turn, helped to return pedals to their starting positions between individual bouts. Passive mode leg motions: When passive mode exercise was performed by TS-rats on the same stepper device, a lifting motor drove the pedal thus over-

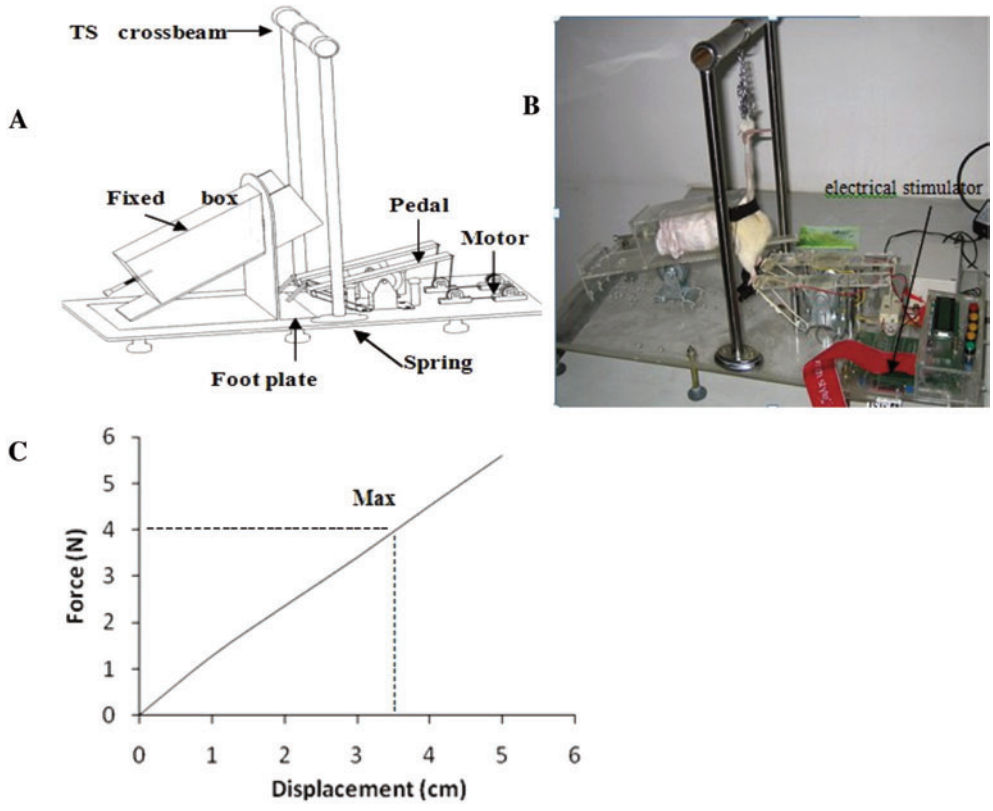


**Figure 1.** Custom-design of a passive or active resistance exercise device (stepper) for the tail-suspended (TS)-rat model. (**A**) Cartoon drawing of stepper construction for use with the TS-rat experimental model. (**B**) Photograph showing TS-rat during exercise on the stepper device in the laboratory. The rat's trunk was placed in a fixed box (30° angle) and hind paws were fixed by adhesives on the stepper footplates. When active mode exercise was performed, training was initiated by short pulses of the electrical arc stimulator. When passive mode exercise was performed, a lifting motor drove the pedal. (**C**) The force of the spring was exerted as the rat's hindlimb was contracting. The maximum force was 4 N corresponding the maximum displacement (3.5 cm).

coming the load of 0-4 N produced by a spring that brought about passive contraction to the TS-rat's hind limb muscles without electric impulse stimulation. This motion was considered as passive mode leg motion. As the original position was always achieved by the spring load, both active and passive mode exercise included passive muscle stretching as final part of each bout. The conscious rats of the TSA and TSP group were trained twice a day (at 9 a.m. and 7 p.m.), with the stepper training approximately lasting about 6 min per day including exactly 40 bouts.

**Electromyogram (EMG) of calf.** A rat's surface EMG detection system was developed as previous described[16]. This system mainly included a four-pin surface electrode attached to rat's hairless calf and discharged via an amplifying-filtering circuit.

**Dual energy X-ray absorptiometry (DXA) of bone.** Before start (day 0) and after end of the TS experiment (day 22, all groups), rats were anaesthetized by 1% pentobarbital sodium (6 ml/kg, i.p.) and bone mineral density (BMD) of entire femur was measured *in vivo* using a clinical DXA machine (Norland XR-36, USA) with small animal software supplementation. For each group, BMD-change to baseline (in%) was calculated as $BMD\%_{change}=(BMD_{22d}-BMD_{0d})/ BMD_{0d}\times100$.

**Micro-computed tomography (μCT) measurements of bone.** Before start (day 0) and after end of experiment (day 22), rats were anaesthetized appropriately (as for DXA measurements) for *in vivo* scan by μCT (SkyScan1076, Belgium). The metaphyses of distal femurs and proximal tibia of rats were scanned as previously reported[17]. Briefly, all scans were in the mode of 70kV X-ray voltage, 143 μA current, 1 mm aluminium filter, 18 μm pixel size, 360° tomographic rotation and a rotation step of 0.6°. The measured region was commenced at the position of 1.898 mm to the growth plate level and extended to the diaphysis for 150 transverse slices (4.745 mm to the growth plate level). All scans were reconstructed with the same parameters. The region of interest (ROI) was delineated by freehand drawing from the same investigator, then trabecular/cortical BMD-change to baseline (in%) was calculated as $BMD\%_{change\text{-}Trab/Cort}=(BMD_{Trab/Cort\text{-}22d}-BMD_{Trab/Cort\text{-}0d})/ BMD_{Trab/Cort\text{-}0d}\times100$. And the trabecular microstructural parameters of both distal femur and proximal tibia were calculated, including: 1) BV/TV (Bone volume fraction), 2) Tb.Th (Trabecular thickness), 3) Tb.N (Trabecular number), and 4) Tb.Sp (Trabecular separation). In addition, cross-sectional area (CSA) of rat whole calf muscles (including m. soleus and m. gastrocnemius) was calculated at 4.745 mm to the growth

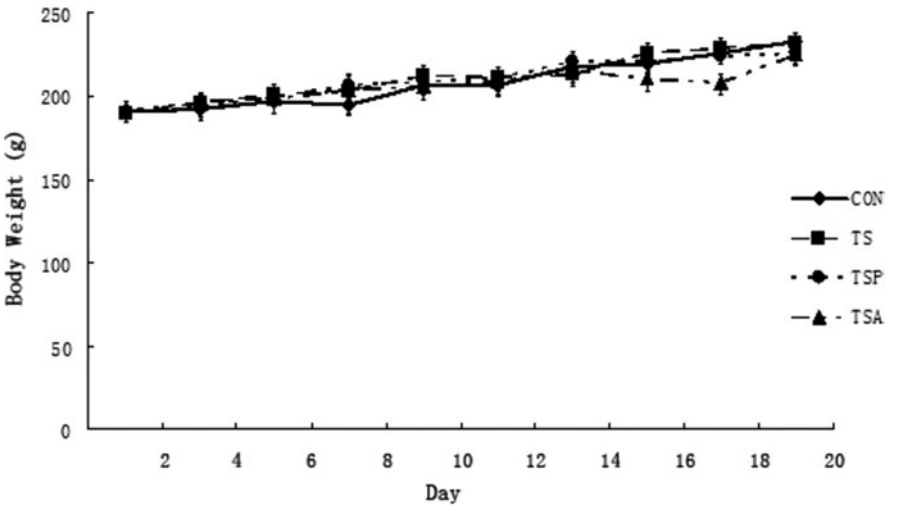


**Figure 2.** Body weights of rats.

plate. All parameters were calculated as change rate similar to BMD, that is $CSA\%_{change\ rate}=(CSA_{22d}-CSA_{0d})/CSA_{0d}\times100$.

**Skeletal muscle.** Following the *in vivo* measures as described above, rats were sacrificed with narcotic overdose (1% Pentobarbital Sodium, 18 ml/kg, i.p.). The soleus muscle (and bones, see below) was immediately excised and frozen rapidly in liquid nitrogen and transferred to -80°C freezer for storage. From the muscle tissue blocks, consecutive series of 8 µm thick cryosections were cut, mounted on coded glass slides, and immunostained for anti-slow (type I) and anti-fast (type II) myosin-heavy chain proteins (sMyHC, fMyHC, Sigma Inc.) as previously reported[18] to verify the two major types of myofibers including hybrids. In addition to anti-MyHCslow and -fast immunostaining, anti-Dystrophin (submembrane protein marker, diluted 1:500) was used in triple-staining protocols on the same cryosections to clearly delineate the outer fiber membrane for accurate size determinations (cross-sectional area, CSA) of slow and fast myofibers. In addition, we used nitric oxide synthase type-1 (NOS1) as a marker of muscle activity[18]. The primary monoclonal or polyclonal antibodies were detected via affinity-purified secondary anti-mouse or anti-goat antibodies labeled with three different fluorescent probes (ALEXA 488, 555 and 615, Molecular Probes Inc., dilutions 1:1000-1:2000). All slides were mounted with coverslips using Vectashield™ mounting medium (Vector Laboratories. CA. USA) and thereafter inspected with a high-resolution three channel laser confocal microscope (Leica TCS SP-2, Germany). Immunostained cryosections from the TS, TSA, TSP and CON animal groups were scanned at identical magnifications (x40 objective) in the same scan sessions using identical scan/image/laser and pixel settings in order to achieve unbiased quantitative pixel-intensity measures and comparison between groups using the software pack of the supplier (Leica # 1234567 software release).

**NOS1 immunofluorescence intensity.** SOL cryosections (8 µm thickness) were double-immunolabelled with anti-NOS1 and anti-fast-myosin heavy chain (fMyHC) antibodies, specific immuno-

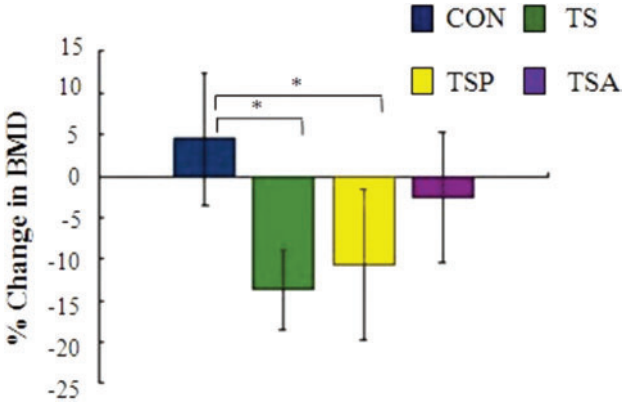


**Figure 3.** Bone mineral density (BMD) changes versus baseline of femora by DXA. *(Values are means ± SD, *p<0.05 compared to CON).*

markers of fast myofibres type-II. The expression of NOS1 in myofibers type I and II was determined by measuring the relative fluorescence intensity of immunostained sarcolemmal membrane structures according to an established immunostaining protocol[18]. Briefly, the area pixel intensity of a selected region of interest (ROI) within the sarcolemma area of about 1.000 $\mu m^2$ of both types I and II myofibers was measured in digitised confocal image scans and expressed as arbitrary units using Leica software (in the range of 0-255 a.u.). At least ten myofibers, of type I and of type II were measured in each cryosection from each animal, each group (for a total of 20,000 $\mu m^2$) in at least three independent immunostaining experiments. Changes of NOS1 intensity was determined by area-based pixel intensity measurements between individual animals from each group (TS, TSA, TSP, CON, n=5 each), and were calculated as percent changing of arbitrary units (a.u.) of each group versus CON (baseline set as 0%). Immunostaining experiments

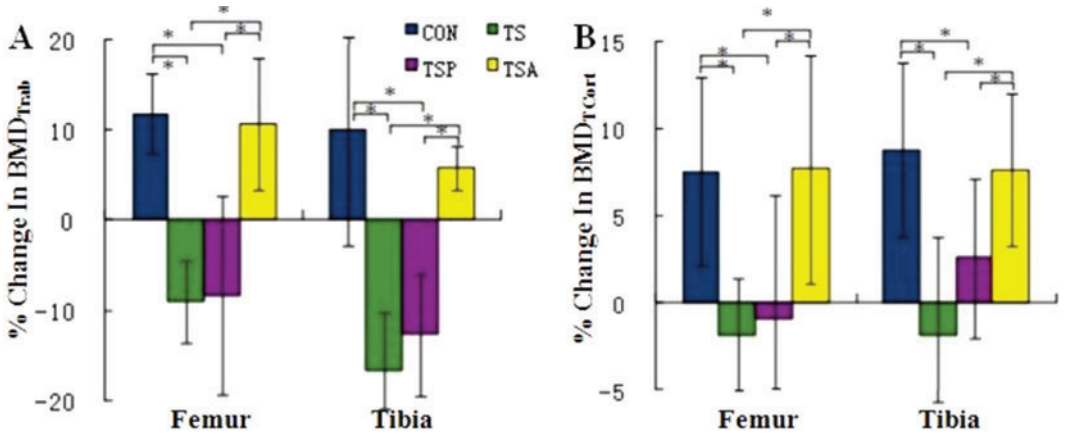


**Figure 4.** Trabecular and cortical BMD (g/cm$^3$) of metaphyses in distal femurs and proximal tibia by μCT. (**A**) trabecular BMD. (**B**) Cortical BMD. *(Values are means ± SD, * p<0.05).*

with secondary detection antibodies only omitting monoclonal primary anti-NOS1 were run as negative controls.

**Bone ash weight.** Femurs and tibias of right hind limbs were excised clean of soft tissues and were treated by modified method as previously described[19]. In details, bones were immersed in solvent (2 vol. chloroform: 1 vol. methanol) to extract fat for 5 days, then dried at 105° in drying oven for 36 h until weight was stable. Dry weight was measured when cooling. All specimens were burned to ash at 700°C in a muffle furnace for 24 h. Then, the ratio of ash weight was calculated as AW%= ash weight/dry weight×100.

**Three-point bending test.** Femurs of left hind limbs were excised clean of soft tissues and wrapped by saline-soaked gauze bandage and then preserved in -20° for three-point bending test. Three-point bending of rat femur in the mediolateral direction was carried out on Shimadzu AG-10KNIS testing machine as previously reported[20]. Briefly, the span was about 20 mm. Before actual testing, a small stabilizing preload (10 N) was applied on the medial surface of the femur at a rate of 0.1 mm/s. The bending load was applied at a rate of 0.2 mm/s until failure of the specimen. The maximum load, stiffness, energy absorption and Young's modulus of the femoral mid shaft were determined and calculated.

*Statistical analysis*

All values were expressed as means ± standard deviation (SD). Statistical analyses were performed between groups with SPSS 13.0 using Univariate and t-test analysis. The level of statistical significance was set at p<0.05.

## Results

*Rat body weight*

The rat body weight was measured during the experiment (Figure 2). There was no significant difference among the general body weight of the four rat groups.

*Bone mineral density (BMD) from DXA and μCT scans*

The DXA-BMD (g/cm$^2$) of femurs decreased significantly in TS and TSP compared to CON animal group p<0.05 (Figure 3). We found no significant differences between TSA and CON. As expected, these results confirmed that tail-suspension resulted in significantly decreased BMD (g/cm$^2$) p<0.05, which could be prevented by active (TSA) rather than passive motion (TSP) exercise countermeasure using the stepper training protocol.

Both trabecular and cortical BMD (mg/cm$^3$) determined by the μCT method in TS and TSP group also decreased significantly compared to either the CON or TSA animal groups p<0.05, while there were no significant differences found between the CON and TSA group (Figure 4).

*Bone microstructural parameters*

We next compared the 3-D reconstructed bone microstructure of CON with TS, TSP and TSA group by the μCT method as further visual documentation of the inner bone microarchitecture (Figure 5A). The 3-D reconstructed microstructure of trabecular bone was significantly deteriorated by TS, and to lesser extend also by TSP, whereas the microstructure was largely preserved by TSA (Figure 5A). All other calculated individual parameters (BV/TV, Tb.Th, Tb.N, and Tb.Sp) showed significant differences between TS and TSP versus CON p<0.05. No differences were found between TSA and CON (Figure 5B-E). However, visible deterioration of normal bone microstructure was present in bones from TS-rats of the passive mode (TSP) exercise group using the same stepper training device as TSA rats.

*Three-point bending test*

In TS rats, stiffness, maximum load, energy absorption and Young's modulus were significantly decreased compared with the CON group using the three-point bending test of bone

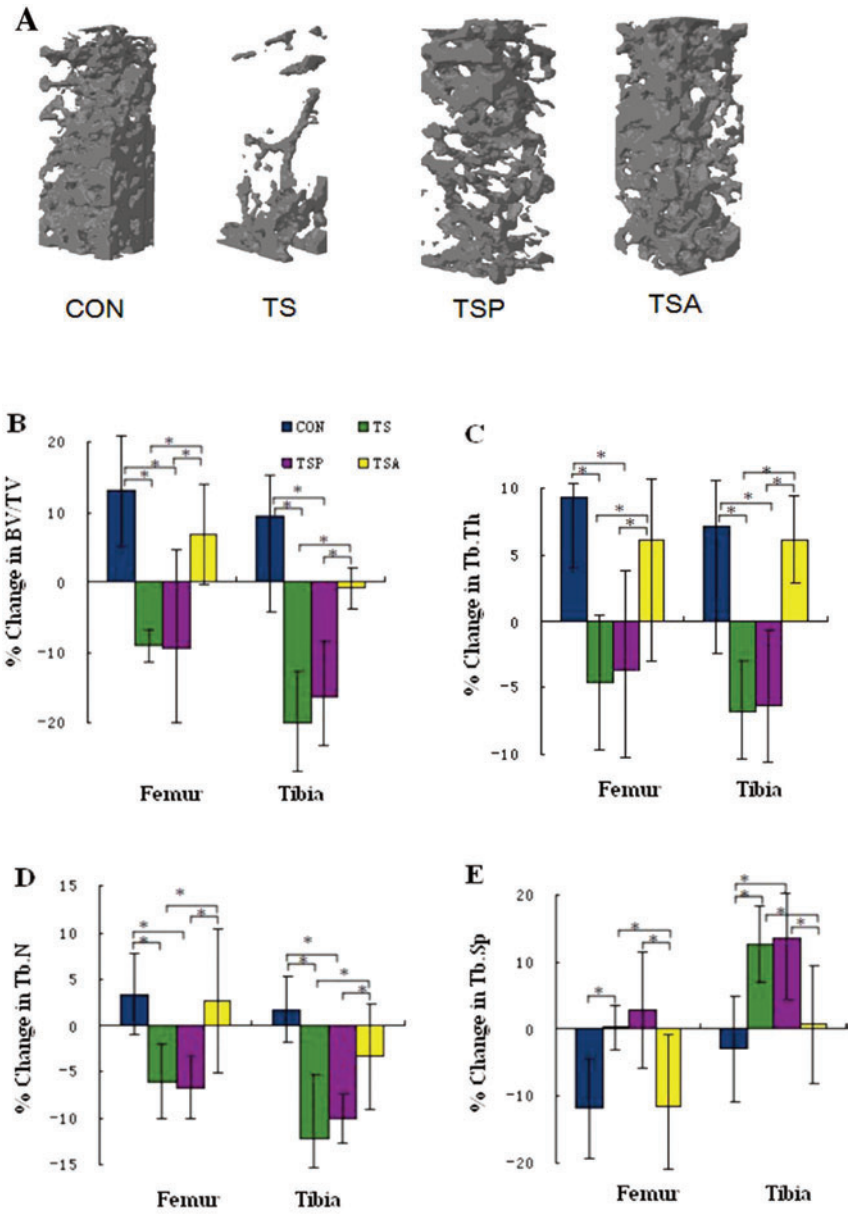


**Figure 5.** Trabecular microstructure of distal femurs and proximal tibias by μCT. (**A**) Three-dimensional (3D) reconstruction of rat trabecular bone of distal femur. The reconstruction region was obtained starting from the position of 1.898 mm (100 slices) to the growth plate level and extended to the diaphysis for 30 transverse slices. (**B**) BV/TV, Bone volume fraction, (**C**) Tb.Th, Trabecular thickness, (**D**) Tb.N, Trabecular number, (**E**) Tb.Sp, Trabecular separation. *(Values are means ± SD, *p<0.05).*

p<0.05 (Table 1). In TSP rats, energy absorption and Young's modulus were significantly different compared with CON rats p<0.05, and all calculated parameters did not show significant differences compared to the TS group. Compared to CON, TSA rat bone values did not show significant changes which were however detectable between TSA vs. TS rats.

*Ash weight measurements*

The ratio of ash weight (AW) of the right femur and tibia is showed in Figure 6. Both TS and TSP group showed significant differences in values compared to CON and TSA rats p<0.05. In addition, there was no significant difference compared to CON in femoral bones.

*Whole Calf Muscle Cross-Sectional Area (CSA)*

Determination of the whole CSA of rat calf muscles was done by μCT in parallel to bone scans to document more general changes in size variations of rat calf muscles between experimental groups in digitized cross-sectional images. The CSA of whole calf muscles (m. soleus, m. gastrocnemius) de-

| Para. | CON | TS | TSP | TSA |
|---|---|---|---|---|
| Stiffness [N/mm] | 186.68±44.081 | 134.61±22.31* | 147.27±10.75 | 183.34±37.55$^{\#}$ |
| Max Load [N] | 91.43±4.12 | 79.02±6.33* | 82.71±8.49 | 92.72±11.16$^{\#}$ |
| Energy Absorp [mJ] | 48.52±7.42 | 32.94±5.45* | 35.78±4.44* | 48.66±7.02$^{\#\,\&}$ |
| Young's Modulus [N/mm$^2$] | 8682.02 ±1466.14 | 6419.92±1469.77* | 6704.34±348.93* | 8809.43±1932.76$^{\#\,\&}$ |

*Values are means ± SD*
**indicates significant difference compared to CON,*
*$^{\#}$indicates significant difference compared to TS,*
*$^{\&}$indicates significant difference compared to TSP.*

**Table 1.** Descriptive data of three-point bending.

creased significantly in TS and TSP compared to CON or TSA $p<0.05$. There was no significant difference found between TSA and CON (Figure 7).

*Myofiber CSA and slow/fast type distribution*

We also determined the histological CSA of individual slow (type I) and fast (type II) myofibers and the ratio of slow/fast hybrid fibers (i.e. immunoreactive for slow and fast MyHC) in cryosections of m. soleus which is a reference slow-type muscle in rats sensitive to gravitational load or unloading (Figure 8). Compared to CON, the CSA of slow (type I) and fast (type II) as well as of the hybrid myofiber subpopulation (Figure 8B, shown as left to right bar clusters plotted against y-axis) was decreased in all groups (TS, TSP and TSA) with the only exception of the fast myofibers in the TSA group (Figure 8B, middle plot clusters) that compared to CON did not show significantly changed CSA values. Compared to TS, slow and fast myofiber CSA was always increased in TSA, but not in TSP group. In addition, the CSA values of the hybrid fibers in the TSA or TSP group were significantly higher compared to those seen in other groups $p<0.05$). The baseline CSA levels of CON rats however were not achieved neither by rats of the TSA nor TSP group (Figure 8).

Compared to CON, the type I (slow) and II (fast) myofiber distribution pattern in m. soleus was significantly altered in all three groups (TS, TSA and TSP) $p<0.05$. Compared to TS only, the myofiber type I and II pattern is comparable to both TSA or TSP. In addition, we also monitored the relative amounts of hybrid fibers (signatures for myofiber type remodeling, Figure 8B, left cluster) in soleus myofibers with no significant changes between TSA and TSP $p<0.05$.

*NOS1 Expression in SOL muscle and its muscle fibers*

As a morphological signature for muscle activity, we analysed the NOS1 fluorescence intensity present at the sarcolemma region of soleus muscle fibers in all experimental groups. NOS1 immunohistochemistry showed strong immunofluorescence at sarcolemma membrane structures in cross-sectioned soleus myofibers in the CON group that was however nearly absent from atrophic myofibers in the TS group, or only faintly expressed in the TSP group as documented by high-res-

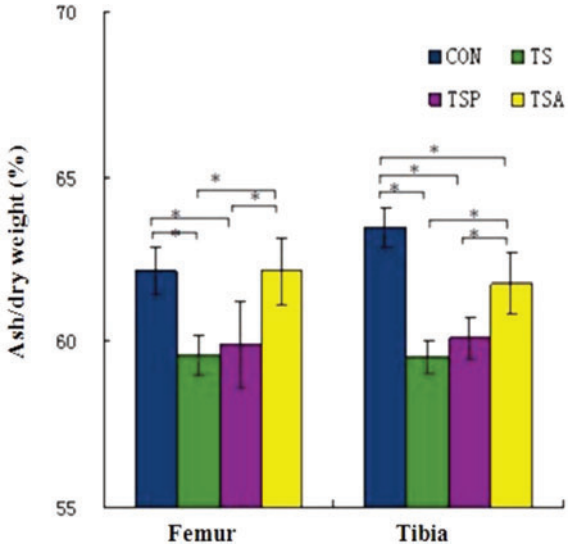


**Figure 6.** Ash weight of right femur and tibia. The proportion of inorganic mineral to total bone weight was expressed as the value in figure. *(Values are means ± SD, *p<0.05).*

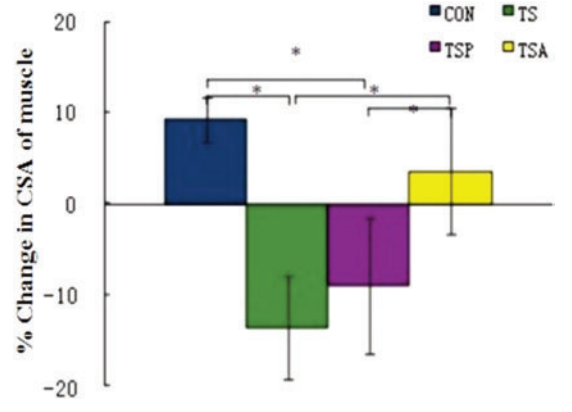


**Figure 7.** Cross-sectional area (CSA) determination of whole rat calf muscle by μCT. *(*p<0.05).*

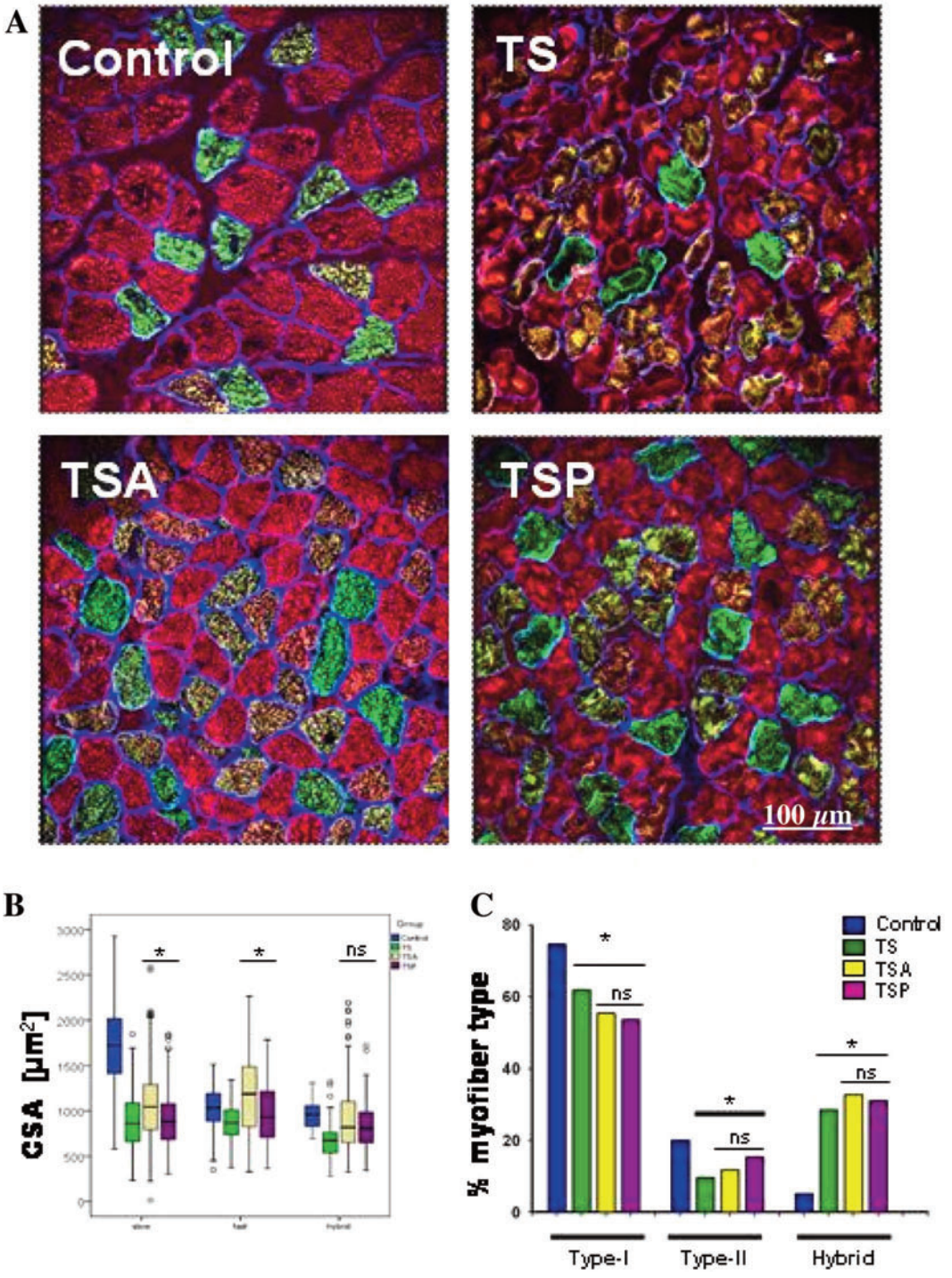


**Figure 8.** Triple-immunostained cryosections showing the pattern of slow (type I, red) and fast (type II, green) myosin heavy chain (MyHC) co-immunostained with membrane marker dystrophin in rat soleus muscle. (**A**) CON (control), TS (tail suspended only), TSA (active exercise), and TSP (passive exercise) group. Note the increased amount of hybrid fibers (yellow label) in TSA group, (**B**) Quantitative determination of myofiber cross-sectional area (CSA) in all four groups (n=5, each group; *p<0.05 TSA vs. TSP or vs. CON). In this plot graph (**B**), 4 experimental groups are plotted as three separate clusters of type 1, type 2, or hybrid fibers (left to right) against CSA values (y-axis, 0-3.000 $\mu m^3$). Each single plot reads as means = single horizontal black line in colored bar; extension of colored body of bar= +/- standard deviation S.D.; longitudinal lines through bar body= max./min. values. (**C**) Quantitative determination of percent change in slow (type I) vs. fast (type II) myofiber type distribution in rat m. soleus in all groups (n=5, each group; *p<0.05). ns=not significant (TSA vs. TSP). Bar represents 100 μm.

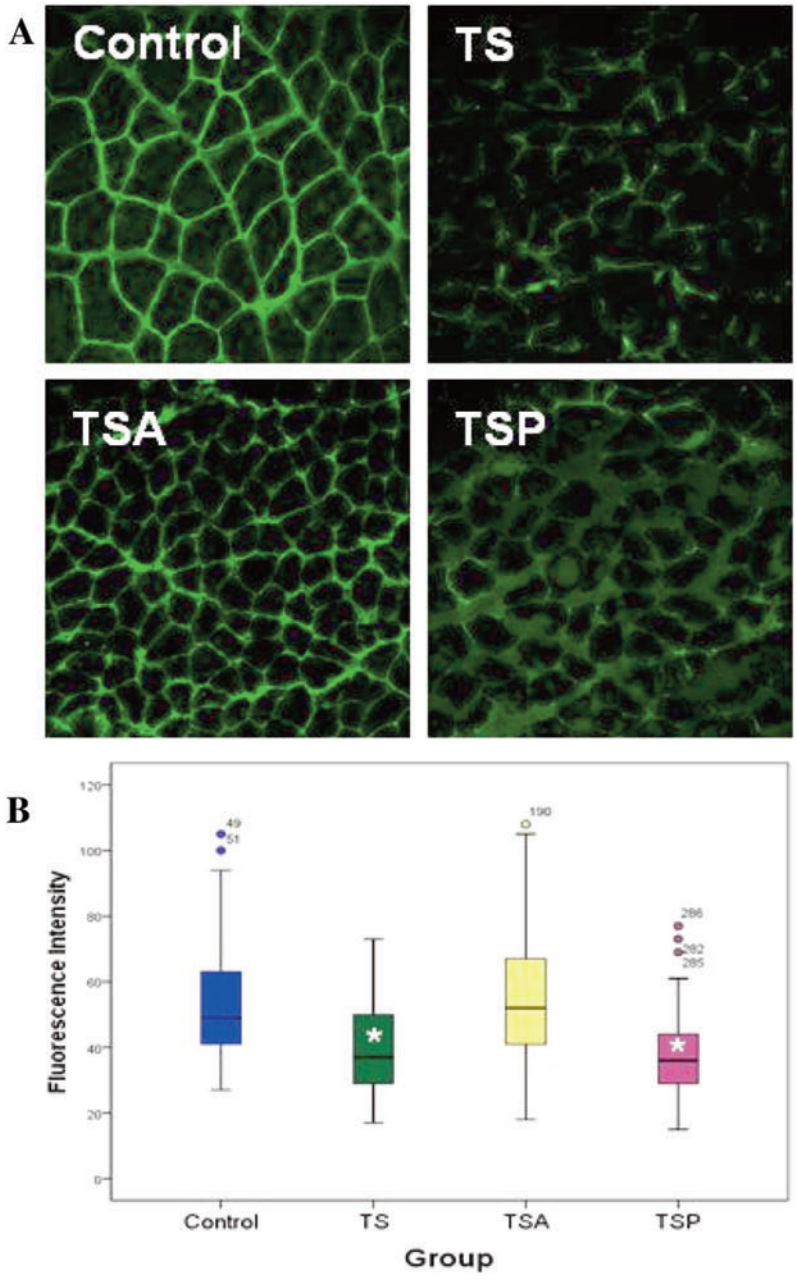


**Figure 9.** Nitric oxide synthase type-1 (NOS1, green) immunoreactivity at sarcolemma membranes of myofibers in rat soleus muscle. (**A**) Control (CON) group (normal cage control), and following 21 days of TS (no exercise), TSA (active mode exercise) and TSP (passive mode exercise). Note that the network-like NOS 1 myofiber membrane pattern (i.e., sarcolemma-associated NOS1) is absent from TS and TSP, but present in TSA rats. (**B**) Plot graph showing quantitative determination of NOS1 fluorescence intensity at sarcolemma membranes in myofibers of all groups (n=5, each group; *p<0.05, t-test). The four experimental groups (Control, TS, TSA TSP) are plotted against NOS1 immunofluorescence intensities (y-axis, 0-120 arbitrary values). Each single plot reads as means = single horizontal black line in colored bar; extension of colored body of bar=+/- standard deviation S.D.; longitudinal lines through bar body=max. / min. values. * significance at p<0.05 vs Control or TSA; Bar (A) represents 100 μm.

olution confocal microscopy (Figure 9). By contrast, soleus myofibers of TSA animals showed a strong sarcolemmal NOS1 immunofluorescence comparable to baseline levels of the CON group (Figure 9). The quantitative pixel image analysis of the immunosignal intensity confirmed reduced sarcolemma NOS1 fluorescence intensities in both TS and TSP compared to the CON group (Figure 9). Our results showed NOS1 myofiber membrane proteins that are both negatively regulated in TS only and positively regulated via active mode (TSA) p<0.05, but not via passive mode (TSP) muscle contractions in rat solei myofibers subjected to 3 weeks of TS following experimental conditions using the same stepper training device.

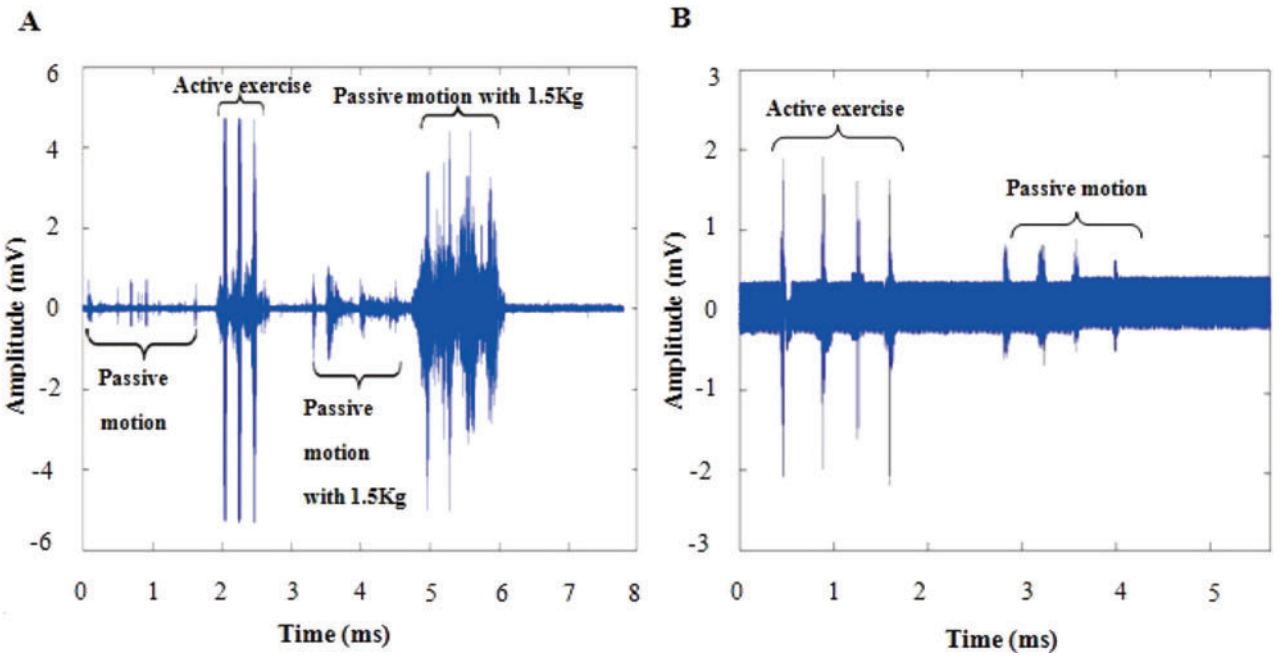


**Figure 10.** EMG of passive and active mode exercise. (**A**) human biceps brachii, (**B**) rat calf muscle (triceps surae). Note amplitude of "passive motion" relative to active exercise is greater for human than rat subjects. Multiple spikes around peak spikes denote auxiliary activation different in human vs. rat muscle (i.e., sharp delineated spikes at passive motions).

*Electromyogram (EMG) of active vs. passive exercise*

The TS-rat active and passive mode exercise performed on the designed stepper device was also monitored in hind limb calf muscles with EMG detection and compared to the signal patterns (mV) in human biceps brachii performing resistive load bouts using 1.5 kg of weight lifting (Figure 10A). The general signal patterns recorded during the two different active or passive TS-rat exercise bouts (Figure 10B) was comparable to the alternating signal patterns recorded from those in the human biceps brachii muscle with differential amplitude peak characteristics (described in Figure 10 legend). Even if direct comparison of muscle activity patterns may be critical between human and animal species, EMG signal patterns in both flexor muscle groups likely monitored active vs. passive muscle activity in general. At least, the results indicated that the active or passive motion exercise for rat was achieved on the custom-made training device.

## Discussion

Since exercise has shown little success in mitigating bone loss from long-duration spaceflight, some researchers tried to combine exercise with other regimens. Recently, a combined exercise and nutrition intervention partially maintained bone mass during spaceflight[21] while Swift et al. discovered that bone formation to resistance training during disuse was blunted by concurrent alendronate treatment[22,23]. Therefore, the development of adequate countermeasures to prevent microgravity-induced musculoskeletal loss and to provide successful postflight rehabilitation is still critical. Based on our present findings, we here altered biodynamic properties of the muscle-bone interface during resistive on-orbit exercise protocols (i.e., reversed active vs passive muscle activation) to counteract musculoskeletal deconditioning of astronauts should be addressed more carefully in future countermeasure developments and protocols.

To further unravel some of the biodynamic mechanisms in the muscle-bone unit of the calf following unloading, we were curious to determine if the mode shift from active vs. passive motion performed in a 1G (control rat group) vs. simulated μG environment (rat hind limb unloading) may provide an important yet underestimated cue to properly counteract weightlessness-induced bone loss and muscle atrophy. The present findings may also help to define improved physical countermeasure regimen not only for future animal research in spaceflight but might also enable the Astronaut in the near future to make use of a biodynamically-based muscle activation in addition to the presently used on-orbit resistive exercise countermeasure protocols to maintain musculoskeletal functions for safe performance control and health in long duration space missions and thereafter.

In ground-based animal experimentation (rats or mice) active mode exercise is usually applied via routine treadmill and/or running wheel exercises or even progressive loading exercise programs such as swimming regimens[24-26]. Likewise, passive motion movements are usually applied following experimental nerve transections (muscle denervation), or alternatively studied in anesthetized rats[27]. Such experimental regimen certainly

cannot be applied to similar human studies in Space for ethical reasons. In order to furthermore study the biodynamic properties in terms of active vs. passive muscle activation in the muscle-bone unit in an experimental animal model simulating microgravity (TS-rat) we designed a novel exercise regimen using a custom-made stepper device that allows for direct comparison between training outcome for a leg muscle-bone unit in two conscious TS-rat groups using either active (TSA) and passive mode (TSP). One limitation of this study is the inability to ensure equal contraction speed during the active vs. passive contraction. This may result in variable contraction-to-rest ratio that might affect the mitigation of bone loss[28]. Therefore, an alternative method should be designed to further investigate the influence of contracted speed in our model.

Our present results from routine bone structural markers provided multiple evidences that BMD, microstructure and biomechanical properties were equally supported by active rather than passive mode exercise to counteract TS-induced osteopenia and thus both exercise modes effectively offset loss in the TS-rat bone quality. Our results from skeletal muscle analysis including activity-dependent biomarkers such as NOS1 expression performed on the soleus calf muscle (a reference slow-type and gravity-sensitive postural calf muscle in rodents and humans) confirmed that structural and molecular parameters were clearly affected by TS and, to lesser extent, also by TSP, but remained largely unchanged following the TSA exercise regimen. Such findings supported the notion that active mode exercise performed on the ground-based rat stepper device clearly prevented major changes in disuse-induced muscle atrophy signatures that, for example, were found in mice calf muscles exposed to long-duration exposure (91 days) to real microgravity on the ISS[29].

Apart from the known principal biomechanical properties of the musculoskeletal system, human performance on the ground (1 G) is based on complex integrative mechanisms of peripheral and central nervous system pathways such as the vestibular/visual input, muscle/tendon receptors and skin afferents or neuroeffector control mechanisms which converge in an adequate performance control that is well-adapted to human normal life on Earth[30,31]. Nevertheless, the motion patterns in human performance in microgravity (μG) appear to be different from the well-known motion patterns performed by the 1 G-adapted locomotor apparatus on Earth[11]. This fact may likely contribute for example to the observed and reported suboptimal outcome of the presently prescribed exercise countermeasure regimen to overcome musculoskeletal deconditioning inflight in Astronauts on the International Space Station[8,9].

Resistive load exercise countermeasure protocols performed by Astronauts on the International Space Station (ISS) on orbit unexpectedly showed weaker effects than previously thought[7,10], suggesting that experience values gained by resistive exercise protocols on Earth also may not be easily extrapolated to on-orbit countermeasure protocols to offset musculoskeletal system deconditioning in human spaceflight. For example, some of the insufficient on-orbit training effects observed with the exercise countermeasure protocols on the ISS[10], may be, at least partly, explained also by the unique biodynamic properties i.e. mechanically active muscle chains (i.e., optimal or habitual coordination of muscle groups and units in open vs. closed chains) between the joint-bone-muscle interfaces as well as by the altered mass inertia (e.g., resistive load provided by the exercise device) used on orbit. However, more sophisticated animal paradigms may be necessary to further unravel differential agonist versus antagonist muscle group activation and to study changed neural activation of agonist/antagonist or synergist muscle groups and the unique vestibular input to the neuromuscular system in-flight versus that observed in 1 G.

In conclusion, using simulated microgravity modeled via hind limb unloading in rats we found that different modes of exercise (active vs passive) actually highlighted different effects on various bone and muscle parameters in rodents using the same stepper device. As expected, active exercise appeared to be more effective than passive motion to prevent disuse-induced bone loss and maladaptation of unloaded rat skeletal muscle supporting the need for spontaneous muscle activation of the soleus to prevent deconditioning of the calf muscle-bone unit. Even though the exact biomechanical properties of the unloaded musculoskeletal system remain to be defined in more details they may likely be altered in a microgravity environment during spaceflight with some impact on the overall outcome of resistive exercise countermeasure inflight in both animals and humans. Therefore, more attention should be paid to the unique biodynamic demands and properties of the muscle-bone interface in case if resistive exercise modes successfully performed on the ground will be used as effective on-orbit countermeasure protocols for animals and possibly also for human spaceflight missions.

*Acknowledgements*

*We thank the National Natural Science Foundation of China (31170897, 11120101001 and 10925208) and the National Basic Research Program of China (2011CB710901) for financial support to this work. We also thank the German Aerospace Board, DLR e.V., Bonn-Oberkassel, Germany for continuous financial support to our work (grant #50WB0821 to D.B.).*

## References

1. Baldwin KM, White TP, Arnaud SB, Edgerton VR, Kraemer WJ, Kram R, Raab-Cullen D, Snow CM. Musculoskeletal adaptations to weightlessness and development of effective countermeasures. Med Sci Sports Exerc 1996; 28:1247-1253.
2. Oser H, Damann V. Physiology research in space and the astronaut countermeasure programme - a potential conflict. J Gravit Physiol 1997;4:P81-83.
3. Hawkey A. The physical price of a ticket into space. J Br Interplanet So 2003;56:152-159.
4. Convertino VA. Clinical aspects of the control of plasma volume at microgravity and during return to one gravity. Med Sci Sports Exerc 1996;28:S4bv-52.

5. Schneider SM, Amonette WE, Blazine K, Bentley J, Lee SM, Loehr JA, Moore AD Jr, Rapley M, Mulder ER, Smith SM. Training with the International Space Station interim resistive exercise device. Med Sci Sports Exerc 2003;35:1935-45.
6. O'toole, Miller-Keane Encyclopedia and Dictionary of Medicine, Nursing, and Allied Health. Vol. 7. 2003, Amsterdam: Saunders.
7. Genc KO, Gopalakrishnan R, Kuklis MM, Maender CC, Rice AJ, Bowersox KD, Cavanagh PR. Foot forces during exercise on the International Space Station. Journal of Biomechanics 2010;43:3020-3027.
8. Cavanagh PR, Genc KO, Gopalakrishnan R, Kuklis MM, Maender CC, Rice AJ. Foot forces during typical days on the international space station. J Biomech 2010;43:2182-2188.
9. Fitts RH, Trappe SW, Costill DL, Gallagher PM, Creer AC, Colloton PA, Peters JR, Romatowski JG, Bain JL, Riley DA. Prolonged space flight-induced alterations in the structure and function of human skeletal muscle fibres. J Physiol 2010;588:3567-3592.
10. Trappe S, Costill D, Gallagher P, Creer A, Peters JR, Evans H, Riley DA, Fitts RH. Exercise in space: human skeletal muscle after 6 months aboard the International Space Station. J Appl Physiol 2009;106:1159-68.
11. Lee SM, Cobb K, Loehr JA, Nguyen D, Schneider SM. Foot-ground reaction force during resistive exercise in parabolic flight. Aviat Space Environ Med 2004;75:405-12.
12. McCrory J, Schwass J, Connell R, Cavanagh P. In-shoe force measurements from locomotion in simulated zero gravity during parabolic flight. Clin Biomech (Bristol, Avon) 1997;12:S7.
13. Morey-Holton ER, Globus RK. Hindlimb unloading of growing rats: a model for predicting skeletal changes during space flight. Bone 1998;22:83S-88S.
14. Morey-Holton ER, Globus RK. Hindlimb unloading rodent model: technical aspects. J Appl Physiol 2002; 92:1367-77.
15. Sun LW, Fan YB, Li DY, Zhao F, Xie T, Yang X, Gu ZT. Pulse electrical arc stimulator based on single-electrode for active exercise in tail-suspension rat. J Cent South Univ T 2008;15: 383-88.
16. Wu YN, Hyland BI, Chen JJ. Biomechanical and electromyogram characterization of neuroleptic-induced rigidity in the rat. Neuroscience 2007;147:183-96.
17. Sun LW, Wang C, Pu F, Li de Y, Niu HJ, Fan YB. Comparative study on measured variables and sensitivity to bone microstructural changes induced by weightlessness between *in vivo* and *ex vivo* micro-CT scans. Calcif Tissue Int 2011;88:48-53.
18. Rudnick J, Puttmann B, Tesch PA, Alkner B, Schoser BG, Salanova M, Kirsch K, Gunga HC, Schiffl G, Luck G, Blottner D. Differential expression of nitric oxide synthases (NOS 1-3) in human skeletal muscle following exercise countermeasure during 12 weeks of bed rest. FASEB J 2004;18:1228-30.
19. Joo YI, Sone T, Fukunaga M, Lim SG, Onodera S. Effects of endurance exercise on three-dimensional trabecular bone microarchitecture in young growing rats. Bone 2003;33:485-93.
20. Sun LW, Fan YB, Li DY, Zhao F, Xie T, Yang X, Gu ZT. Evaluation of the mechanical properties of rat bone under simulated microgravity using nanoindentation. Acta Biomater 2009;5:3506-11.
21. Smith SM, Heer MA, Shackelford LC, Sibonga JD, Ploutz-Snyder L, Zwart SR. Benefits for bone from resistance exercise and nutrition in long-duration spaceflight: Evidence from biochemistry and densitometry. J Bone Miner Res 2012;27:1896-906.
22. Swift JM, Swift SN, Nilsson MI, Hogan HA, Bouse SD, Bloomfield SA. Cancellous bone formation response to simulated resistance training during disuse is blunted by concurrent alendronate treatment. J Bone Miner Res 2011;26:2140-50.
23. Swift JM, Nilsson MI, Hogan HA, Sumner LR, Bloomfield SA. Simulated resistance training during hindlimb unloading abolishes disuse bone loss and maintains muscle strength. J Bone Miner Res 2010;25:564-74.
24. Cornachione A, Cação-Benedini LO, Martinez EZ, Neder L, Cláudia Mattiello-Sverzut A. Effects of eccentric and concentric training on capillarization and myosin heavy chain contents in rat skeletal muscles after hindlimb suspension. Acta Histochem 2011;113:277-282.
25. Ishihara A KF, Ishioka N, Oishi H, Higashibata A, Shimazu T, Ohira Y. Effects of running exercise during recovery from hindlimb unloading on soleus muscle fibers and their spinal motoneurons in rats. Neurosci Res 2004; 48:119-127.
26. Renno AC, Silveira Gomes AR, Nascimento RB, Salvini T, Parizoto N. Effects of a progressive loading exercise program on the bone and skeletal muscle properties of female osteopenic rats. Exp Gerontol 2007;42:517-22.
27. Agata N SN, Inoue-Miyazu M, Kawakami K, Hayakawa K, Kobayashi K, Sokabe M. Repetitive stretch suppresses denervation-induced atrophy of soleus muscle in rats. Muscle Nerve 2009;39:456-462.
28. Lam H, Hu M, Qin YX. Alteration of contraction-to-rest ratio to optimize trabecular bone adaptation induced by dynamic muscle stimulation. Bone 2011;48:399-405.
29. Sandona D, Desaphy JF, Camerino GM, Bianchini E, Ciciliot S, Danieli-Betto D, Dobrowolny G, Furlan S, Germinario E, Goto K, Gutsmann M, Kawano F, Nakai N, Ohira T, Ohno Y, Picard A, Salanova M, Schiffl G, Blottner D, Musaro A, Ohira Y, Betto R, Conte D, Schiaffino S. Adaptation of mouse skeletal muscle to long-term microgravity in the MDS mission. PLoS One 2012; 7:e33232.
30. Edgerton VR, Roy RR. Neuromuscular adaptation to actual and simulated weightlessness. Adv Space Biol Med 1994;4:33-67.
31. Kozlovskaya IB, Grigoriev AI. Russian system of countermeasures on board of the International Space Station (ISS): the first results. Acta Astronaut 2004;55:233-7.